HHS Public Access

Author manuscript

Hepatology. Author manuscript; available in PMC 2024 May 31.

Published in final edited form as:

Hepatology. 2023 September 01; 78(3): 896–910. doi:10.1097/HEP.0000000000000019.

Conventional type 1 dendritic cells protect against gut barrier disruption via maintaining *Akkermansia muciniphila* in alcoholic steatohepatitis

Liuyi Hao[1], **Wei Zhong**[1,2], **Jongmin Woo**[1], **Xiaoyuan Wei**[3], **Hao Ma**[4], **Haibo Dong**[1], **Wei Guo**[1], **Xinguo Sun**[1], **Ruichao Yue**[1], **Jiangchao Zhao**[3], **Qibin Zhang**[1,5], **Zhanxiang Zhou**[1,2]

[1]Center for Translational Biomedical Research, Kannapolis, North Carolina, USA

[2]Department of Nutrition, Kannapolis, North Carolina, USA

[5]Department of Chemistry and Biochemistry, University of North Carolina at Greensboro, North Carolina Research Campus, Kannapolis, North Carolina, USA

[3]Department of Animal Science, Division of Agriculture, University of Arkansas, Fayetteville, Arkansas, USA

[4]Department of Epidemiology, Tulane University School of Public Health and Tropical Medicine, New Orleans, Louisiana, USA

Abstract

Background and Aims: Alcohol-perturbed gut immune homeostasis is associated with the development of alcoholic liver disease (ALD). However, the role of intestinal dendritic cells (DCs) in ALD progression is still unknown. This study aimed to investigate the cellular and molecular mechanisms through which intestinal DCs respond to alcohol exposure and contribute to the pathogenesis of ALD.

Approach and Results: After 8 weeks of alcohol consumption, the number of basic leucine zipper transcription factor ATF-like 3 (*Batf3*)-dependent conventional type 1 DCs (cDC1s) was dramatically decreased in the intestine but not the liver. cDC1 deficient *Batf3* knockout mice along with wild-type mice were subjected to chronic-binge ethanol feeding to determine the role of intestinal cDC1s reduction in ALD. cDC1s deficiency exacerbated alcohol-induced gut barrier disruption, bacterial endotoxin translocation into the circulation, and liver injury. Adoptive transfer of cDC1s to alcohol-fed mice ameliorated alcohol-mediated gut barrier dysfunction and liver injury. Further studies revealed that intestinal cDC1s serve as a positive regulator of *Akkermansia*

Correspondence Zhanxiang Zhou, Center for Translational Biomedical Research and Department of Nutrition, the University of North Carolina at Greensboro, North Carolina Research Campus, 600 Laureate Way, Suite 2203, Kannapolis, NC 28081. z_zhou@uncg.edu.

AUTHOR CONTRIBUTIONS

Zhanxiang Zhou, and Liuyi Hao conceived and designed research; Liuyi Hao, Jongmin Wu, Xiaoyuan Wei, Wei Zhong, Xinguo Sun, Haibo Dong, Wei Guo, Jiangchao Zhao, Qibin Zhang, and Zhanxiang Zhou performed experiments and data analysis. Hao Ma and Liuyi Hao performed statistical analyses. All the authors participated in manuscript preparation.

CONFLICTS OF INTEREST

No potential conflicts of interest relevant to this article are reported.

Supplemental Digital Content is available for this article. Direct URL citations appear in the printed text and are provided in the HTML and PDF versions of this article on the journal's website, www.hepjournal.com.

muciniphila (*A. muciniphila*). Oral administration of *A. muciniphila* markedly reversed alcoholic steatohepatitis in mice. Mechanistic studies revealed that cDC1s depletion exacerbated alcohol-downregulated intestinal antimicrobial peptides which play a crucial role in maintaining *A. muciniphila* abundance, by disrupting the IL-12-interferon gamma signaling pathway. Lastly, we identified that intestinal cDC1s were required for the protective role of *Lactobacillus reuteri* in alcoholic steatohepatitis.

Conclusions: This study demonstrated that cDC1s protect alcohol-induced liver injury by maintaining *A. muciniphila* abundance in mice. Targeting cDC1s may serve as a promising therapeutic approach for treating ALD.

INTRODUCTION

Alcoholic liver disease (ALD) is one of the most common forms of chronic liver disease worldwide.[1] While alcohol induces deleterious effects on the liver, it also disrupts intestinal epithelial integrity as well as antimicrobial responses, resulting in increased gut permeability, bacterial translocation, and release of pathogen-associated molecular patterns (PAMPs) into circulation.[2,3] Translocation of PAMPs (eg, bacterial endotoxin) from the intestinal tract to the liver represents crucial inflammatory signaling that triggers the hepatic proinflammatory response and subsequent injury.[4]

Alcohol consumption is associated with enteric dysbiosis and intestinal bacterial overgrowth in both alcohol-fed mice and patients with ALD.[5] ALD can be transmitted via fecal microbiota,[6] suggesting a causal link between dysbiosis and the development of ALD. *Akkermansia muciniphila* (*A. muciniphila*) is one of the most abundant members of the human gut microbiota. During the progression of ALD, the reduction of *A. muciniphila* is intimately associated with liver damage in both human and mice.[7] Mice treated with *A. muciniphila* efficiently improved intestinal barrier integrity and reversed alcohol-induced liver injury.[7] Moreover, *A. muciniphila* administration reduced cardiovascular disease[8] and obesity,[9] making *A. muciniphila* a promising probiotic candidate for maintaining gut health. However, the precise mechanisms underlying how alcohol reduces the abundance of *A. muciniphila* in the pathogenesis of ALD have not been well defined.

Dendritic cells (DCs) are antigen-presenting cells that comprise 2 major subsets: conventional DCs (cDCs) and plasmacytoid DC. Intestinal DCs are highly heterogeneous but collectively generate both regulatory and effector T-cell responses which are essential for maintaining intestinal immune homeostasis.[10] Intestinal cDCs development is specifically regulated by distinct transcriptional factors. Basic leucine zipper transcription factor ATF-like 3 (*Batf3*) and interferon regulatory factor 8 (*Irf8*) are essential for $CD103^{+}CD11b^{-}$ conventional type 1 DCs (cDC1s) development in the intestine.[11,12] Whereas, interferon regulatory factor 4 (*Irf4*) and notch receptor 2 (*Notch2*) are critical for intestinal $CD103^{+}CD11b^{+}$ conventional type 2 DCs (cDC2s) development.[13] *Batf3*-dependent cDC1 has been recognized as the major producer of IL-12 among all DC subsets and are essential in driving protective interferon gamma (IFN-γ)-secreting T helper type 1 (Th1) and CD8 T cells immunity upon infection.[11,14] Mice lacking cDC1s exhibited dramatically decreased intestinal IFN-γ levels and enhanced susceptibility to dextran sodium sulfate-induced colitis.

[15,16] We previously reported that alcohol-impaired intestinal IFN-γ signaling provides an explanation for alcohol-induced gut antimicrobial dysfunction, *A. muciniphila* reduction, gut barrier disruption, and liver injury.[17] However, how alcohol affects intestinal DCs and how perturbed intestinal DCs may mediate alcohol-induced dysbiosis, gut barrier dysfunction, and PAMPs translocation in the development of ALD remain largely unclear.

MATERIALS AND METHODS

Animals and chronic alcohol feeding

C57BL/6J mice and *Batf3* knockout (KO) (*Batf3*$^{-/-}$) mice were purchased from the Jackson Laboratory (Bar Harbor, ME). All mice were housed under specific pathogen-free conditions with controlled temperature and 12-hour light/dark circle. For the collection of tissue samples, mice were anesthetized with inhalational isoflurane. All animal studies were conducted by following the protocol approved by the North Carolina Research Campus Institutional Animal Care and Use Committee. Twelve weeks old male mice were fed with the Lieber-DeCarli liquid diets containing alcohol (alcohol-fed; AF) or isocaloric maltose dextrin control liquid diet (pair-fed; PF) for 8 weeks (NIAAA model with some modifications). The ethanol (Ethyl alcohol 190 proof, Product # 493538; Sigma-Aldrich, St. Louis, MO) content (%, v/v) in the diet was 4.5% (24% ethanol-derived calories in the diet) for the first 2 weeks and gradually increased by 0.37% (2% ethanol-derived calories in the diet) every 2 weeks, reaching 5.6% (30% ethanol-derived calories in the diet) for the last 2 weeks. Food intake was measured daily, and the amount of food given to the pair-fed mice was the same as what the alcohol-fed mice consumed in the previous day. Four hours before tissue collection, the AF mice were administrated with 1 dose of ethanol at 4 g/kg and the PF mice with isocaloric maltose dextrin.

Other materials and methods used in this study are described in the Supplemental Materials and Methods, and in Supplemental Tables 1-3 (http://links.lww.com/HEP/A20).

RESULTS

Chronic alcohol consumption leads to a reduction of intestinal Batf3-dependent CD103^{+}CD11b^{-} cDC1s in mice

The effects of alcohol on intestinal and hepatic DCs were assessed. Chronic alcohol feeding increased the number of total cDCs in the small intestinal lamina propria (SILP, Figure 1A), large intestine LP (LILP, Figure 1A), and payer's patch (PP; Supplemental Figure 1A, http://links.lww.com/HEP/A20) in mice. However, the number of hepatic cDCs was not affected (Figure 1A and Supplemental Figure 1B, http://links.lww.com/HEP/A20). To determine whether alcohol consumption alters DC functions in the gut, ileal cDCs were isolated. Principal components analysis revealed that quantified proteins could distinguish 2 groups with 49.1% of the variance (Supplemental Figure 2A, http://links.lww.com/HEP/A20). We discovered 62 differentially expressed proteins with statistical significance (Figure 1B and Supplemental Figure 2B http://links.lww.com/HEP/A20). Functional enrichment analysis of downregulated proteins in the AF group showed that alcohol perturbed the

function of migration, invasion and glycolysis metabolism in cDCs (Supplemental Figure 2C http://links.lww.com/HEP/A20).

Intestinal cDCs are a heterogeneous population of cells and we next measured the effects of alcohol on intestinal cDCs subsets. Surprisingly, the number and frequency of $CD103^+CD11b^-$ cDC1 DCs were robustly decreased in SILP (Figure 1C), LILP (Figure 1C), and PP (Supplemental Figure 1A http://links.lww.com/HEP/A20) after chronic alcohol feeding, while no change was found in hepatic $CD103^+CD11b^-$ DCs (Figure 1C). The ileal mRNA levels of cDC1 markers, including *Batf3*, C-Type Lectin Domain Containing 9A (*Clec9A*), and X-C Motif Chemokine Receptor 1 (*Xcr1*) were all reduced by alcohol feeding (Figure 1D). The number of resident $CD8\alpha^+CD11b^-$ cDC1s in mesenteric lymph nodes (MLN), whose development relies on *Batf3*, was also decreased by alcohol (Figure 1C). Intriguingly, in contrast to the cDC1 reduction, alcohol feeding significantly increased the number of cDC2s in the SILP, LILP, PP, and MLN (Supplemental Figure 1C, http://links.lww.com/HEP/A20).

cDC1s are the major IL-12 secreting cDC subset.[14] As shown in Figure 1E, intestinal cDCs isolated from the AF mice produced less IL-12 protein upon CpG ODN1585 stimulation than that from the PF mice. The ileal IL-12 protein levels were also decreased in the AF mice (Figure 1E). Furthermore, the frequency of ileal $CD45^+IL\text{-}12R^+$ cells was markedly lower in the AF mice (Supplemental Figure 3A, http://links.lww.com/HEP/A20). Intestinal cDC1s play an essential role in regulating Th1 ($CD4^+IFN\text{-}\gamma^+$) and $CD8^+IFN\text{-}\gamma^+$ T cells development via IL-12 signaling. Indeed, the proportion of both ileal Th1 and $CD8^+IFN\text{-}\gamma^+$ T cells were all reduced by alcohol feeding (Figure 1F). The protein (Figure 1F) and mRNA levels (Supplemental Figure 3B, http://links.lww.com/HEP/A20) of ileal IFN-γ were markedly reduced in the AF mice. Moreover, the mRNA levels of *Ifn-γ* downstream targets, including C-X-C Motif Chemokine Ligand 9 (*Cxcl9*), indoleamine 2,3-dioxygenase (*Ido*), and interferon gamma-induced protein 10 (*Ip-10*), were all decreased in the ileum of AF mice compared with PF mice (Supplemental Figure 3C, http://links.lww.com/HEP/A20). The protein levels of ileal phosphorylated signal transducer and activator of transcription 3 (p-STAT3), which are controlled by IFN-γ, were also markedly reduced in the AF mice (Supplemental Figure 3D, http://links.lww.com/HEP/A20).

Lack of cDC1s exacerbates alcohol-induced intestinal tight junction disruption and PAMPs translocation in mice.

To determine the role of cDC1s in the pathogenesis of ALD, $Batf3^{-/-}$ mice were subjected to eight weeks of alcohol feeding. The ileal mRNA levels of *Batf3* were undetectable after KO (Supplemental Figure 4A, http://links.lww.com/HEP/A20). The ileal mRNA levels of *Xcr1*, a marker of cDC1s, were also dramatically decreased in the $Batf3^{-/-}$ mice (Supplemental Figure 4A, http://links.lww.com/HEP/A20). *Batf3* KO significantly decreased the number of $CD103^+CD11b^-$ cDC1s in the SILP (Figure 2A) and $CD8\alpha^+CD11b^-$ cDC1s in the MLN (Supplemental Figure 4B, http://links.lww.com/HEP/A20), respectively. Moreover, IL-12 secretion by ileal DCs upon CpG ODN1585 stimulation was significantly damped by *Batf3* KO (Supplemental Figure 4C, http://links.lww.com/HEP/A20). The frequency of ileal Th1 (Figure 2B), $CD8^+IFN\text{-}\gamma^+$ T cells (Supplemental Figure 4D,

http://links.lww.com/HEP/A20), and ileal IFN-γ (Figure 2C and Supplemental Figure 4E, http://links.lww.com/HEP/A20) and *Ip-10* mRNA levels (Figure 2C) were all dramatically decreased in the *Batf3*$^{-/-}$ mice, regardless of alcohol feeding. Interestingly, *Batf3* KO also exacerbated alcohol-increased ileal CD103^{+}CD11b^{+} cDC2s, Th17 cells, and the mRNA levels of *Il-17a* (Supplemental Figure 4F, http://links.lww.com/HEP/A20).

We next examined whether intestinal cDC1s reduction was involved in alcohol-perturbed intestinal epithelial tight junction. As shown in Figure 2D, alcohol-decreased mRNA levels of ileal *Occludin*, zonula occludens-1 (*Zo-1*), and *Claudin1* were all exacerbated in *Batf3*$^{-/-}$ mice. Alcohol-decreased protein levels of ileal OCCLUDIN and ZO-1 were also enhanced by *Batf3* KO (Figure 2D). Alcohol-induced disruption of intestinal barrier integrity facilitates PAMPs translocation to the blood and liver. Indeed, alcohol-increased plasma and hepatic endotoxin levels were also exacerbated by cDC1s deletion (Figure 2E).

However, the mRNA and protein levels of ileal TNF-α (Figure 2F and Supplemental Figure 5, http://links.lww.com/HEP/A20), IL-6, and C-C Motif Chemokine Ligand 2 (CCL2) (Supplemental Figure 5, http://links.lww.com/HEP/A20) were comparable between the alcohol-fed wild-type (WT) mice and *Batf3*$^{-/-}$ mice.

Lack of Batf3-dependent cDC1s exacerbates alcohol-induced hepatic inflammation, steatosis, ER stress, and liver injury

We previously reported that hepatic lipocalin-2 (LCN2) elevation was associated with PAMPs translocation in both alcohol-fed mice and patients with alcoholic hepatitis.[2] As shown in Figure 3A and Supplemental Figure 6A, http://links.lww.com/HEP/A20, alcohol-increased the mRNA and protein levels of hepatic LCN2 were exacerbated in the *Batf3*$^{-/-}$ mice. Deletion of *Batf3* also enhanced alcohol-increased hepatic p-STAT3 (Figure 3A) and NF-κB protein levels (Supplemental Figure 6A, http://links.lww.com/HEP/A20).

Flow cytometry analysis showed that alcohol increased the frequency of hepatic neutrophils were exacerbated by *Batf3* KO (Figure 3B). Correspondingly, alcohol-increased mRNA levels of hepatic chemokine (C-X-C motif) ligand 1 (*Cxcl1*) were enhanced by *Batf3* KO (Figure 3B). Compared with WT/AF mice, KO/AF mice also exhibited a markedly higher number of M1 macrophages in the liver (Figure 3B). Although alcohol feeding alone did not affects the mRNA and protein levels of hepatic CCL2 and TNF-α in the WT mice, *Batf3* KO significantly increased the mRNA and protein levels of these genes after alcohol feeding (Figure 3B; Supplemental Figure 6B, http://links.lww.com/HEP/A20). The KO/AF mice also displayed a higher proportion of infiltrated monocytes in the liver (Supplemental Figure 6C, http://links.lww.com/HEP/A20).

Alcohol-induced lipid droplet accumulation in the liver was exacerbated by *Batf3* KO (Figures 3C, E). Alcohol feeding elevated the serum levels of alanine aminotransferase (ALT) and aspartate aminotransferase in both the WT mice and *Batf3*$^{-/-}$ mice with the latter having significantly higher values (Figure 3C). Deletion of *Batf3* also worsened alcohol-induced hepatic ER stress, which is evidenced by increased protein levels of activating transcription factor 4 (ATF4) and C/EBP homologous protein (CHOP) (Figure 3D). Furthermore, the KO/AF mice exhibited a higher mortality rate during the alcohol

feeding period (Figure 3F). However, hepatic protein levels of alcohol metabolizing enzymes, including alcohol dehydrogenases and cytochrome P450 2E1, and serum ethanol levels were comparable between WT/AF mice and KO/AF mice (Supplemental Figure 7, http://links.lww.com/HEP/A20).

Adoptive transfer of cDC1 ameliorates alcohol-induced intestinal barrier disruption, PAMPs translocation, and liver injury

Since loss of cDC1s exacerbated alcohol-induced liver injury, we next determined whether adoptive transfer of cDC1s could reverse the disease progression. As shown in Figure 4A, $MHCII^+CD11c^+CD103^+Clec9A^+$ cDC1s, which were selectively and efficiently generated from bone marrow, were adoptively transferred to AF mice via intravenous injection. Adoptive transfer of cDC1s reversed alcohol-impaired ability of IL-12 secretion in ileal DCs (Figure 4A). Alcohol-decreased ileal IFN-γ protein levels (Figure 4A) and the frequency of ileal Th1 and $CD8^+IFN\text{-}\gamma^+$ T cells (Supplemental Figure 8A, http://links.lww.com/HEP/A20) were reversed by cDC1s adoptive transfer. cDC1s adoptive transfer also increased the mRNA levels of *Ifn-γ* in the liver (Supplemental Figure 8C, http://links.lww.com/HEP/A20). cDC1s transfer ameliorated alcohol-reduced the mRNA and protein levels of ileal OCCLUDIN and ZO-1 (Figure 4B; Supplemental Figure 8B, http://links.lww.com/HEP/A20). Accordingly, both the serum and hepatic levels of endotoxin were reduced after cDC1 transfer (Figure 4C). Moreover, alcohol-increased the hepatic frequencies of neutrophils (Figure 4D), the number of $F4/80^+CD80^+CD206^-$ M1 macrophages (Supplemental Figure 8D, http://links.lww.com/HEP/A20), and the mRNA levels of *Cxcl1 and Lcn2* (Figure 4D) were all attenuated by cDC1s adoptive transfer. Alcohol-induced lipid accumulation in the liver was reversed by cDC1s adoptive transfer (Figure 4E). Mice with cDC1s administration also alleviated alcohol-elevated serum ALT levels (Figure 4F).

Batf3-dependent cDC1s control A. muciniphila abundance via regulating IFN gamma signaling in the gut

The cecal microbiome was analyzed by metagenomic sequencing of the 16S rRNA gene. Loss of intestinal cDC1s perturbed the gut microbial configuration (Figure 5A). At the family level, the relative abundance of Verrucomicrobiaceae was significantly decreased after chronic alcohol feeding, and this effect was further exacerbated by *Batf3* KO (Figure 5A; Supplemental Figure 9A, http://links.lww.com/HEP/A20). The abundance of *A. muciniphila* was also decreased by alcohol feeding and *Batf3* KO, while the KO/AF mice displayed the lowest abundance of *A. muciniphil*a (Figure 5B). The relative abundances of Enterobacteriaceae and Enterococcus were significantly higher in the KO/AF mice than the WT/AF mice (Supplemental Figure 9B, http://links.lww.com/HEP/A20). However, both alcohol and *Batf3* KO did not significantly affect the relative abundance of Lactobacillaceae (Figure 5A; Supplemental Figure 9A, http://links.lww.com/HEP/A20).

We previously reported that intestinal antimicrobial peptides (AMPs) are the essential regulators of the *A. muciniphila* abundance in ALD.[2,17] As shown in Figure 5C, the mRNA levels of ileal defensin alpha 5 (*Def*a5) were significantly lower in $Batf3^{-/-}$ mice than that in WT mice on either a control or alcohol diet. Moreover, alcohol-decreased mRNA levels of ileal regenerating islet-derived protein 3β (R*eg3β*) and *Reg3γ* were

all exacerbated by *Batf3* KO (Supplemental Figure 10A, http://links.lww.com/HEP/A20). Furthermore, alcohol-decreased intestinal *A. muciniphila* abundance was ameliorated by cDC1s transfer (Figure 5D). Consistently, alcohol-decreased ileal mRNA levels of *Defa5* (Figure 5E), *Reg3β*, and *Reg3γ* (Supplemental Figure 10C, http://links.lww.com/HEP/A20) were all reversed by cDC1s transfer.

Intestinal STAT3 signaling plays an essential role in maintaining AMPs levels.[17] As shown in Supplemental Figure 10B, http://links.lww.com/HEP/A20, *Batf3* KO sufficiently led to a reduction of ileal p-STAT3 protein levels. Furthermore, alcohol-decreased ileal p-STAT3 protein levels were exacerbated by *Batf3* KO (Supplemental Figure 10B, http://links.lww.com/HEP/A20), while cDC1 adoptive transfer ameliorated alcohol-decreased ileal p-STAT3 protein levels in mice (Supplemental Figure 10D, http://links.lww.com/HEP/A20).

Our previous study indicated that IFN-γ controls the abundance of *A. muciniphila* via mediating intestinal STAT3-AMPs signaling. To evaluates whether IFN-γ was involved in *Batf3* KO-mediated *A. muciniphila* reduction, low dose of IFN-γ (300 ng/mouse) was administrated to the WT/AF mice and *Batf3* KO/AF mice. The mRNA levels of intestinal *Ip-10* and *Ido*, were increased by IFN-γ administration (Supplemental Figure 11A, http://links.lww.com/HEP/A20). The protein levels of p-STAT3 were reversed by IFN-γ in both WT/AF mice and KO/AF mice (Supplemental Figure 11B, http://links.lww.com/HEP/A20). As shown in Figure 5F, IFN-γ completely reversed alcohol-reduced abundance of intestinal *A. muciniphila* in both WT mice and mice KO mice. Furthermore, the *Batf3* KO-exacerbated ileal AMPs reduction was totally reversed by IFN-γ administration (Figure 5F).

To evaluate whether IL-12 signaling was involved in *Batf3* KO-mediated IFN-γ and *A. muciniphila* reduction, we administrated IL-12 to both WT mice and $Batf3^{-/-}$ mice fed with alcohol chronically. IL-12 strongly reversed alcohol-mediated and *Batf3* KO-mediated reduction of ileal *Ifn-γ*, *Ido*, and *Ip-10* expression (Supplemental Figure 11C, http://links.lww.com/HEP/A20). Alcohol-decreased mRNA levels of ileal *Defa5*, *Reg3β*, and *Reg3γ* (Supplemental Figure 11D, http://links.lww.com/HEP/A20) and the protein levels of p-STAT3 (Supplemental Figure 11E, http://links.lww.com/HEP/A20) were also reversed by IL-12 administration. Concomitantly, the alcohol-reduced abundance of *A. muciniphila* was eversed by IL-12 in both WT/AF and KO/AF mice (Supplemental Figure 11F, http://links.lww.com/HEP/A20).

Oral *A. muciniphila* administration ameliorates the detrimental effects of Batf3 KO on the tight junction functions and PAMPs translocation

To determine whether the reduction of *A. muciniphila* was involved in the detrimental effects of cDC1s depletion in ALD, *A. muciniphila* was orally administrated to alcohol-fed WT mice and $Batf3^{-/-}$ mice. As shown in Figure 6A. *A. muciniphila* administration ameliorated the detrimental effects of cDC1s deficiency on alcohol-induced intestinal epithelial tight junction disruption. In accordance, alcohol-increased plasma and hepatic endotoxin levels were reversed by *A. muciniphila* administration in both WT mice and $Batf3^{-/-}$ mice (Figure 6B). Alcohol-increased mRNA (Figure 6C) and protein levels (Figure 6C; Supplemental Figure 12A, http://links.lww.com/HEP/A20) of hepatic LCN2

and the protein levels of hepatic p-STAT3 (Figure 6D) were suppressed by *A. muciniphila* administration in both WT mice and *Batf3*$^{-/-}$ mice. However, *A. muciniphila* administration did not affect the number of cDC1s in the small intestine (Figure 6E). Furthermore, the mRNA (Figure 6F) and protein (Supplemental Figure 12B, http://links.lww.com/HEP/A20) levels of ileal IFN-γ, and the mRNA levels of ileal *Defa5* and *Reg3β* (Supplemental Figure 12C, http://links.lww.com/HEP/A20) were not affected by *A. muciniphila* administration.

Oral *A. muciniphila* supplementation ameliorates the detrimental effects of Batf3 KO on alcohol-induced liver injury

We next explored the effect of *A. muciniphila* on alcohol and *Batf3* KO-induced liver injury. As shown in Figure 7A, *A. muciniphila* administration reversed *Batf3* KO-enhanced neutrophil infiltration into the liver in alcohol-fed mice. *A. muciniphila* supplementation reduced the mRNA levels of hepatic *Cxcl1*, *Ccl2*, *Tnf-α*, and *Il-1β* (Figure 7B). *A. muciniphila* administration reversed alcohol-elevated serum ALT levels in both WT mice and *Batf3*$^{-/-}$ mice (Figure 7C). The detrimental effect of *Batf3* KO on alcohol-induced lipid accumulation was also ameliorated by *A. muciniphila* (Figures 7D, E). Alcohol-induced hepatic ATF4 and CHOP protein levels in the WT/AF mice and KO/AF mice were almost completely reversed by *A. muciniphila* administration (Figure 7F).

Batf3-dependent cDC1s are involved in the protective effect of Lactobacillus reuteri on alcohol-induced PAMPs translocation and liver injury

Previous study demonstrated that *Lactobacillus (L.) reuteri* supplementation attenuates alcohol-induced intestinal tight junction disruption and liver injury in mice.[18] Interestingly, we found that *L. reuteri* significantly reversed alcohol-decreased numbers of ileal cDC1s in WT mice but not in *Batf3*$^{-/-}$ mice (Figure 8A). The alcohol-impaired IL-12 secretion by ileal cDCs from WT mice was significantly reversed by *L. reuteri* administration, whereas this effect was diminished in DCs from *Batf3*$^{-/-}$ mice (Supplemental Figure 13A, http://links.lww.com/HEP/A20). Alcohol-mediated ileal IFN-γ reduction was reversed by *L. reuteri* administration in WT mice but not in *Batf3*$^{-/-}$ mice (Figure 8B; Supplemental Figure 13B). *L. reuteri* also reversed alcohol-reduced ileal Th1 and IFN-γ secreting CD8 T cells in WT mice but not in KO mice (Supplemental Figure 13C, http://links.lww.com/HEP/A20). Furthermore, the protective effect of *L. reuteri* on alcohol-decreased ileal *Defa5* (Figure 8B) and *Reg3γ* (Supplemental Figure 13D, http://links.lww.com/HEP/A20) mRNA levels were abolished by *Batf3* KO. *L. reuteri* significantly restored the abundance of *A. muciniphila* in WT/AF mice but not in KO/AF mice (Figure 8C). The protective effects of *L. reuteri* on alcohol-disrupted intestinal epithelial tight junctions were abrogated in the *Batf3*$^{-/-}$ mice (Figure 8C; Supplemental Figure 13E, http://links.lww.com/HEP/A20). *L. reuteri* treatment decreased the plasma endotoxin levels (Figure 8C), hepatic *Lcn2* mRNA levels (Supplemental Figure 13F, http://links.lww.com/HEP/A20), and neutrophils infiltration (Figure 8E) in WT/AF mice but not in *Batf3* KO/AF mice. Alcohol-induced hepatic lipid accumulation (Figure 8F; Supplemental Figure 13G, http://links.lww.com/HEP/A20) and liver injury (Figure 8D) were ameliorated by *L. reuteri* in the WT/AF mice but not in the KO/AF mice.

DISCUSSION

ALD is tightly linked to the disruption of gut innate and adaptive immunity in patients as well as in experimental animal models.[19,20] However, the role of alcohol on intestinal DCs was largely unknown. The present study demonstrated that intestinal *Batf3*-dependent cDC1s play a protective role in the development of ALD by maintaining gut permeability via regulation of *A. muciniphila* abundance. We observed that the number of cDC1s was dramatically decreased in the gut but not in the liver of mice after alcohol consumption. By using cDC1s deficiency mice and cDC1s adoptive transfer approach, we identified that cDC1s protect against alcohol-induced gut tight junction disruption, PAMPs translocation into the circulation, hepatic inflammation, and subsequent liver injury. Investigations of the underlying mechanisms further revealed that *A. muciniphila* reduction, resulting from intestinal IL-12-IFN-γ signaling perturbation and subsequent antimicrobial responses disruption, was mechanistically involved in cDC1s deficiency-mediated tight junction disruption and liver injury in ALD. We also found that intestinal cDC1s were involved in the protective effects of *L. reuteri* on alcohol-induced hepatic steatohepatitis in mice (Figure 8G).

Crosstalk between gut immune cells, commensals, and colonic epithelia is required for the proper function of the intestinal mucosal barrier.[21,22] cDCs play an essential role in shaping the intestinal immune response by orchestrating immune tolerance and protective immunity in the host.[23] cDC1s, a master regulator of Th1 response, are characterized by cell surfer marker XCR1, CD8α, and CLEC9A. Their development is highly dependent on the expression of the transcription factors *Batf3* and *Irf8*.[24] cDC2s, defined by the cell surface expression of CD11b and CD172α, exhibit variable dependence on *Irf4* and *Notch2* signaling and mediate Th17 cell development.[25] Previous study demonstrated that intestinal *Irf4*-dependent cDC2s promote postoperative ileus by enhancing gut inflammation.[26] In contrast, cDC1s as a protective DC subset that prevents the onset and evolution of age-related and diet-related obesity and associated morbidities.[27] Lack of cDC1s promotes hepatic steatosis progression towards steatohepatitis in response to high sucrose diet and methionine and choline-deficient diet in mice.[28] However, the role of cDCs in the development of ALD is still unclear. In this study, our results showed that the number of intestinal cDC1s was dramatically reduced after chronic alcohol consumption in mice. cDC1s depletion exacerbated alcohol-perturbed tight junction functions. In line with our results, mice lack intestinal cDC1s but not cDC2s enhanced dextran sodium sulfate-induced tight junction disruption.[15] Previously studies demonstrated that tight junction disruption facilitated the translocation of PAMPs (eg, bacterial endotoxin) from the intestinal tract to the circulation, which triggers a hepatic proinflammatory response.[29-31] Indeed, our results showed that lack of cDC1 exacerbates alcohol-induced PAMPs translocation, hepatic *Lcn2* and *Cxcl1* induction, neutrophils infiltration, and liver injury. These results suggest that cDC1s are serving as a gatekeeper for intestinal barrier integrity in mice. However, we cannot rule out the effect of liver $CD103^{+}CD11b^{-}$ DCs in the development of ALD, due to whole-body *Batf3*$^{-/-}$ mice also displaying $CD103^{+}CD11b^{-}$ cDC1 depletion in the liver. A previous study demonstrated that alcohol-increased intestinal Th17 immune response plays a detrimental in the development of ALD.[32] Interestingly, we found that the number of

cDC2s, the frequency of Th17 cells, and the mRNA levels of *Il-17a* in the ileum were all increased by alcohol consumption and *Batf3* KO. Therefore, future studies are needed to explore whether intestinal cDC2-controlled Th17/IL-17A signaling was involved in the pathogenesis of cDC1 deficiency-enhanced liver injury.

Nowadays, *A. muciniphila* is widely considered a novel potential candidate to improve metabolic disorders.[33,34] Ethanol exposure diminishes intestinal *A. muciniphila* abundance in both mice and humans and can be recovered in experimental ALD by oral supplementation.[7] Notably, *A. muciniphila* significantly promotes intestinal barrier integrity and ameliorates experimental ALD.[7] An outer membrane protein of *A. muciniphila*, Amuc_1100, which interacts with host toll-like receptor 2, was recently found to have an important role in promoting gut barrier integrity through the upregulation of tight junction proteins and is thought to be involved in the beneficial properties shown by this bacterium in patients with obesity.[35] Although the beneficial effects of *A. muciniphila* were well documented in multiple types of disease, the upstream regulator of *A. muciniphila* is still obscure. In this study, we found that *Batf3*-dependent cDC1s control the abundance of *A. muciniphila* in mice. Our results indicated that *Batf3*-dependent cDC1s protect against alcohol-induced tight junction disruption, PAMPs translocation, hepatic inflammation, and liver damage by maintaining *A. muciniphila* abundance. This notion is supported by several findings. First, *Batf3*$^{-/-}$ mice exhibit significantly decreased *A. muciniphila* abundance regardless of alcohol feeding. Second, oral *A. muciniphila* administration significantly ameliorates *Batf3* KO-exacerbated tight junction disruption, PAMPs translocation, and liver inflammation in chronic alcohol-fed mice. Third, adoptive transfer of cDC1 efficiently ameliorates alcohol-induced *A. muciniphila* reduction, gut barrier dysfunction, and subsequent liver inflammation. Finally, *A. muciniphila* supplementation strongly reversed alcohol-induced steatosis, ER stress, and liver injury in both WT mice and *Batf3*$^{-/-}$ mice. Collectively, these results suggest *Batf3* KO-mediated *A. muciniphila* reduction mechanistically links to alcohol-induced tight junction disruption, PAMPs translocation, and hepatic steatohepatitis.

Recently, our group revealed that alcohol-decreased intestinal IFN-γ expression led to *A. muciniphila* reduction by modulating AMPs secretion in mice.[17] IFN-γ restoration significantly reversed alcohol-induced *A. muciniphila* abundance reduction, tight junction disruption, and liver inflammation by enhancing intestinal AMP expression via activating STAT3 signaling.[17] Notably, intestinal epithelial-specific STAT3 deletion-mediated AMPs reduction can be strongly reversed by IFN-γ administration.[17] However, the mechanisms underlying how alcohol mediates intestinal IFN-γ reduction are still unclear. IL-12 is a master upstream regulator of IFN-γ and plays important role in both innate and adaptive immunity.[36,37] IL-12 drives Th1 responses by augmenting IFN-γ production, which is the key molecule for the clearance of intracellular pathogens.[38] Indeed, *Leishmania major* infection-mediated local Th1 immunity was severely hindered in cDC1 deficiency mice due to impaired IL-12 production.[14] Adoptive transfer of WT but not IL-12p40−/− cDCs significantly improved anti-*Leishmania major* response in infected *Batf3*$^{-/-}$ mice,[14] suggesting that IL-12 production by *Batf3*-dependent CD103^{+}CD11b^{-} DCs is crucial for the maintenance of local Th1 immunity. IL-12 was also influencing the level of IFN-γ production by CD8^{+} T cells while IL-23 had little effect on this response.[39] In this study,

our data indicated that mice lacking of cDC1s displayed dramatically decreased IFN-γ levels in the gut and this effect can be totally recovered by IL-12 administration. We found that both low doses of IL-12 and IFN-γ administration restored alcohol-decreased *A. muciniphila* abundance in WT mice and *Batf3*$^{-/-}$ mice, respectively. This effect was accomplished by restoring ileal p-STAT3 protein levels, AMP expression levels, and tight junction functions in alcohol-fed mice. Previously studies demonstrated that the levels of intestinal AMPs, including DEFA5, REG3β, and REG3γ, were dramatically decreased after alcohol consumption.[3] Overexpression of intestinal *Reg3γ* protects alcohol-induced gut dysbiosis, bacterial translocation, and liver damage.[3] A previous study showed that α-defensin 5 (HD5) treatment significantly reversed alcohol-induced *A. muciniphila* reduction, gut barrier disruption, liver inflammation, and liver injury,[2] suggesting alcohol-perturbed AMP secretion is a pathological factor for *A. muciniphila* reduction. It is noteworthy that *A. muciniphila* was able to restore the expression of specific AMPs.[40] However, in this study, alcohol-mediated AMP secretion reduction was not affected by *A. muciniphila* administration, indicating that *A. muciniphila*-altered AMPs expression may largely depend on the type of disease. Collectively, our results demonstrated that perturbed IL-12-IFN-γ-STAT3-AMPs signaling is mechanically involved in cDC1 deficiency-mediated *A. muciniphila* reduction in ALD.

Liver is the major organ responsible for ethanol metabolism, while such metabolism also occurs in the gastrointestinal tract. Interestingly, our results showed that chronic alcohol feeding significantly decreased the number of cDC1 in the gut but not in the liver in mice, suggesting alcohol alone may not directly control the cDC1 number. The human body's largest population of microorganisms resides in the intestine. Considering gastrointestinal tract microbiota and its metabolites modulate immune cells' developments and functions, we hypothesized that gut dysbiosis might be involved in alcohol-induced intestinal cDC1 reduction. Lactobacillus is a type of probiotic bacteria and is believed to play important role in the development and maintenance of the mucosal immune cells of the host.[41,42] A previous study demonstrated that *L. rhamnosus GG* significantly increased the frequency of intestinal cDC1 but decreased cDC2 in the gut,[43] suggesting *L. rhamnosus GG* differently controls intestinal DC subset development. Lactobacillus administration also increased *A. muciniphila* abundance in the fecal content of the DIO mice by ~100 fold.[44] *L. reuteri*, a type of probiotic which was widely used in the clinical treatment of digestive system diseases, can activate DCs that skew T cells toward Th1 polarization via IL-12 signaling.[45] Considering *L. reuteri* administration protects alcohol-induced tight junction disruption and liver injury,[18] we hypothesized that cDC1 may be involved in the beneficial role of *L. reuteri* in the pathogenesis of ALD. Here, we found that *L. reuteri* strongly increased the number of ileal cDC1 in the WT mice but not in *Batf3*$^{-/-}$ mice. Concomitantly, the alcohol-impaired ability of IL-12 secretion in ileal DCs was markedly reversed by *L. reuteri* administration, whereas this effect was completely abolished in cDC1 from *Batf3*$^{-/-}$ mice. In line with that, *L. reuteri*-increased ileal IFN-γ levels and frequency of Th1 cells were all abrogated by cDC1 depletion. The abundance of *A. muciniphila* and the expression of intestinal AMPs were all increased by *L. reuteri* supplementation in alcohol-fed mice, whereas these effects were diminished in cDC1 deficiency mice. Consistently, the protective effects of *L. reuteri* on alcohol-induced tight junction disruption and liver inflammation

were also abrogated by *Batf3* KO. Taken together, these results suggest that cDC1 was a downstream target of *L. reuteri* in the development of ALD.

In summary, we have identified that the intestinal cDC1s act as an active orchestrator and therapeutic target in ALD. Our data demonstrate that cDC1s protect against alcohol-induced tight junction disruption, PAMPs translocation, hepatic inflammation, and liver injury in mice. Mechanistically, cDC1s maintain *A. muciniphila* abundance in the gut via regulating the STAT3-AMP pathway through IL-12-IFN-γ signaling. Based on these findings, targeting intestinal cDC1s might have therapeutic potential for the treatment of ALD.

Supplementary Material

Refer to Web version on PubMed Central for supplementary material.

ACKNOWLEDGMENTS

The authors thank Dr. Rennan Feng, Dr. Qiuju Zhang, and Dr. Huan Xu at the Harbin Medical University for the statistical analysis assistance.

Financial support

This research was supported by the National Institutes of Health grants R01AA018844 (Zhanxiang Zhou) and R01AA020212 (Zhanxiang Zhou & Qibin Zhang).

DATA ACCESS

The raw data and peptide sequencing results were uploaded to the PRIDE database. Access No. PXD033700.

Abbreviations:

A. muciniphila	*Akkermansia muciniphila*
AF	alcohol-fed
ALD	alcoholic liver disease
ALT	alanine aminotransferase
AMPs	antimicrobial peptides
ATF4	activating transcription factor 4
Batf3	basic leucine zipper transcription factor ATF-like 3
CCL2	C-C Motif Chemokine Ligand 2
cDCs	conventional dendritic cells
CHOP	C/EBP homologous protein
Clec9A	C-Type Lectin Domain Containing 9A (Clec9A)
CXCL1	chemokine (C-X-C motif) ligand 1

CXCL9	C-X-C Motif Chemokine Ligand 9
Defa5	defensin alpha 5
ER	endoplasmic reticulum
H&E	hematoxylin and eosin
IHC	Immunohistochemistry
IDO	indoleamine 2,3-dioxygenase
IF	Immunofluorescence
IFN-γ	interferon gamma
IP-10	interferon gamma-induced protein 10
IRF8	interferon regulatory factor 8
L. reuteri	*Lactobacillus reuteri*
LCN2	lipocalin-2
LILP	large intestinal lamina propria
LPS	Lipopolysaccharide
MLN	mesenteric lymph nodes
Notch2	notch receptor 2
PAMPs	pathogen-associated molecular patterns
PCoA	principal coordinates analysis
PF	pair-fed
PP	payer’s patch
Reg3β	regenerating islet-derived protein 3β
SILP	small intestinal lamina propria
STAT3	signal transducer and activator of transcription 3
TG	Triglyceride
XCR1	X-C Motif Chemokine Receptor 1
ZO-1	zonula occludens-1

REFERENCES

1. Gao B, Bataller R. Alcoholic liver disease: pathogenesis and new therapeutic targets. Gastroenterology. 2011;141:1572–85. [PubMed: 21920463]

2. Zhong W, Wei X, Hao L, Lin T, Yue R, Sun X, et al. Paneth cell dysfunction mediates alcohol-related steatohepatitis through promoting bacterial translocation in mice: role of zinc deficiency. Hepatology. 2020;71:1575–91. [PubMed: 31520476]

3. Wang L, Fouts DE, Starkel P, Hartmann P, Chen P, Llorente C, et al. Intestinal REG3 lectins protect against alcoholic steatohepatitis by reducing mucosa-associated microbiota and preventing bacterial translocation. Cell Host Microbe. 2016;19:227–39. [PubMed: 26867181]

4. Shao T, Zhao C, Li F, Gu Z, Liu L, Zhang L, et al. Intestinal HIF-1alpha deletion exacerbates alcoholic liver disease by inducing intestinal dysbiosis and barrier dysfunction. J Hepatol. 2018;69:886–95. [PubMed: 29803899]

5. Yan AW, Fouts DE, Brandl J, Stärkel P, Torralba M, Schott E, et al. Enteric dysbiosis associated with a mouse model of alcoholic liver disease. Hepatology. 2011;53:96–105. [PubMed: 21254165]

6. Shasthry SM. Fecal microbiota transplantation in alcohol related liver diseases. Clin Mol Hepatol. 2020;26:294–301. [PubMed: 32570299]

7. Grander C, Adolph TE, Wieser V, Lowe P, Wrzosek L, Gyongyosi B, et al. Recovery of ethanol-induced *Akkermansia muciniphila* depletion ameliorates alcoholic liver disease. Gut. 2018;67:891–901. [PubMed: 28550049]

8. Li J, Lin S, Vanhoutte PM, Woo CW, Xu A. *Akkermansia muciniphila* protects against atherosclerosis by preventing metabolic endotoxemia-induced inflammation in Apoe−/− Mice. Circulation. 2016;133:2434–46. [PubMed: 27143680]

9. Depommier C, Everard A, Druart C, Plovier H, Van Hul M, Vieira-Silva S, et al. Supplementation with *Akkermansia muciniphila* in overweight and obese human volunteers: a proof-of-concept exploratory study. Nat Med. 2019;25:1096–3. [PubMed: 31263284]

10. Stagg AJ, Hart AL, Knight SC, Kamm MA. The dendritic cell: its role in intestinal inflammation and relationship with gut bacteria. Gut. 2003;52:1522–9. [PubMed: 12970149]

11. Hildner K, Edelson BT, Purtha WE, Diamond M, Matsushita H, Kohyama M, et al. Batf3 deficiency reveals a critical role for CD8alpha+ dendritic cells in cytotoxic T cell immunity. Science. 2008;322:1097–0. [PubMed: 19008445]

12. Sichien D, Scott CL, Martens L, Vanderkerken M, Van Gassen S, Plantinga M, et al. IRF8 transcription factor controls survival and function of terminally differentiated conventional and plasmacytoid dendritic cells, respectively. Immunity. 2016;45:626–40. [PubMed: 27637148]

13. Briseno CG, Satpathy AT, Davidson JT, Ferris ST, Durai V, Bagadia P, et al. Notch2-dependent DC2s mediate splenic germinal center responses. Proc Natl Acad Sci USA. 2018;115:10726–31. [PubMed: 30279176]

14. Martinez-Lopez M, Iborra S, Conde-Garrosa R, Sancho D. Batf3-dependent CD103+ dendritic cells are major producers of IL-12 that drive local Th1 immunity against Leishmania major infection in mice. Eur J Immunol. 2015;45:119–29. [PubMed: 25312824]

15. Muzaki AR, Tetlak P, Sheng J, Loh SC, Setiagani YA, Poidinger M, et al. Intestinal CD103(+)CD11b(−) dendritic cells restrain colitis via IFN-gamma-induced anti-inflammatory response in epithelial cells. Mucosal Immunol . 2016;9:336–51. [PubMed: 26174764]

16. Arnold IC, Zhang X, Artola-Boran M, Fallegger A, Sander P, Johansen P, et al. BATF3-dependent dendritic cells drive both effector and regulatory T-cell responses in bacterially infected tissues. PLoS Pathog. 2019;15:e1007866. [PubMed: 31188899]

17. Yue R, Wei X, Zhao J, Zhou Z, Zhong W. Essential role of IFN-gamma in regulating gut antimicrobial peptides and microbiota to protect against alcohol-induced bacterial translocation and hepatic inflammation in mice. Front Physiol. 2020;11:629141. [PubMed: 33536944]

18. Zheng TX, Pu SL, Tan P, Du YC, Qian BL, Chen H, et al. Liver metabolomics reveals the effect of *Lactobacillus reuteri* on alcoholic liver disease. Front Physiol. 2020;11:595382. [PubMed: 33281626]

19. Zhou Z, Zhong W. Targeting the gut barrier for the treatment of alcoholic liver disease. Liver Res. 2017;1:197–207. [PubMed: 30034913]

20. Mendes BG, Schnabl B. From intestinal dysbiosis to alcohol-associated liver disease. Clin Mol Hepatol. 2020;26:595–605. [PubMed: 32911590]

21. Okumura R, Takeda K. Roles of intestinal epithelial cells in the maintenance of gut homeostasis. Exp Mol Med. 2017;49:e338. [PubMed: 28546564]

22. Powell N, Walker MM, Talley NJ. The mucosal immune system: master regulator of bidirectional gut-brain communications. Nat Rev Gastroenterol Hepatol. 2017;14:143–59. [PubMed: 28096541]
23. Grainger JR, Askenase MH, Guimont-Desrochers F, da Fonseca DM, Belkaid Y. Contextual functions of antigen-presenting cells in the gastrointestinal tract. Immunol Rev. 2014;259:75–87. [PubMed: 24712460]
24. Stagg AJ. Intestinal dendritic cells in health and gut inflammation. Front Immunol. 2018;9:2883. [PubMed: 30574151]
25. Schlitzer A, Sivakamasundari V, Chen J, Sumatoh HR, Schreuder J, Lum J, et al. Identification of cDC1- and cDC2-committed DC progenitors reveals early lineage priming at the common DC progenitor stage in the bone marrow. Nat Immunol. 2015;16:718–28. [PubMed: 26054720]
26. Pohl JM, Gutweiler S, Thiebes S, et al. Irf4-dependent CD103(+) CD11b(+) dendritic cells and the intestinal microbiome regulate monocyte and macrophage activation and intestinal peristalsis in postoperative ileus. Gut. 2017;66:2110–0. [PubMed: 28615301]
27. Hernandez-Garcia E, Cueto FJ, Cook ECL, Redondo-Urzainqui A, Charro-Zanca S, Robles-Vera I, et al. Conventional type 1 dendritic cells protect against age-related adipose tissue dysfunction and obesity. Cell Mol Immunol. 2022;19:260–75. [PubMed: 34983945]
28. Heier EC, Meier A, Julich-Haertel H, Djudjaj S, Rau M, Tschernig T, et al. Murine CD103(+) dendritic cells protect against steatosis progression towards steatohepatitis. J Hepatol. 2017;66:1241–50. [PubMed: 28108233]
29. Ma TY, Nguyen D, Bui V, Nguyen H, Hoa N. Ethanol modulation of intestinal epithelial tight junction barrier. Am J Physiol. 1999;276:G965–74. [PubMed: 10198341]
30. Zhong W, McClain CJ, Cave M, Kang YJ, Zhou Z. The role of zinc deficiency in alcohol-induced intestinal barrier dysfunction. Am J Physiol Gastrointest Liver Physiol. 2010;298:G625–33. [PubMed: 20167873]
31. Hao L, Sun Q, Zhong W, Zhang W, Sun X, Zhou Z. Mitochondria-targeted ubiquinone (MitoQ) enhances acetaldehyde clearance by reversing alcohol-induced posttranslational modification of aldehyde dehydrogenase 2: a molecular mechanism of protection against alcoholic liver disease. Redox Biol. 2018;14:626–36. [PubMed: 29156373]
32. Chu S, Sun R, Gu X, Chen L, Liu M, Guo H, et al. Inhibition of sphingosine-1-phosphate-induced Th17 cells ameliorates alcohol-associated steatohepatitis in mice. Hepatology. 2021;73:952–67. [PubMed: 32418220]
33. Cheng D, Xie MZ. A review of a potential and promising probiotic candidate-*Akkermansia muciniphila*. J Appl Microbiol. 2021;130:1813–22. [PubMed: 33113228]
34. York AA muciniphila boosts metabolic health. Nat Rev Microbiol. 2021;19:343.
35. Plovier H, Everard A, Druart C, Depommier C, Van Hul M, Geurts L, et al. A purified membrane protein from *Akkermansia muciniphila* or the pasteurized bacterium improves metabolism in obese and diabetic mice. Nat Med. 2017;23:107–3. [PubMed: 27892954]
36. Wysocka M, Kubin M, Vieira LQ, Ozmen L, Garotta G, Scott P, et al. Interleukin-12 is required for interferon-gamma production and lethality in lipopolysaccharide-induced shock in mice. Eur J Immunol. 1995;25:672–. [PubMed: 7705395]
37. Hamza T, Barnett JB, Li B. Interleukin 12 a key immunoregulatory cytokine in infection applications. Int J Mol Sci. 2010;11:789–806. [PubMed: 20479986]
38. Conejero L, Khouili SC, Martinez-Cano S, Izquierdo HM, Brandi P, Sancho D. Lung CD103+ dendritic cells restrain allergic airway inflammation through IL-12 production. JCI Insight. 2017;10:2.
39. Henry CJ, Ornelles DA, Mitchell LM, Brzoza-Lewis KL, Hiltbold EM. IL-12 produced by dendritic cells augments CD8+ T cell activation through the production of the chemokines CCL1 and CCL17. J Immunol. 2008;181:8576–4. [PubMed: 19050277]
40. Everard A, Belzer C, Geurts L, Ouwerkerk JP, Druart C, Bindels LB, et al. Cross-talk between *Akkermansia muciniphila* and intestinal epithelium controls diet-induced obesity. Proc Natl Acad Sci USA. 2013;110:9066–71. [PubMed: 23671105]
41. Di Cerbo A, Palmieri B, Aponte M, Morales-Medina JC, Iannitti T. Mechanisms and therapeutic effectiveness of lactobacilli. J Clin Pathol. 2016;69:187–203. [PubMed: 26578541]

42. Wang Y, Kirpich I, Liu Y, Ma Z, Barve S, McClain CJ, et al. Lactobacillus rhamnosus GG treatment potentiates intestinal hypoxia-inducible factor, promotes intestinal integrity and ameliorates alcohol-induced liver injury. Am J Pathol. 2011;179:2866–75. [PubMed: 22093263]

43. Jiang Y, Ye L, Cui Y, Yang G, Yang W, Wang J, et al. Effects of Lactobacillus rhamnosus GG on the maturation and differentiation of dendritic cells in rotavirus-infected mice. Benef Microbes. 2017;8:645–56. [PubMed: 28670908]

44. Zhou K Strategies to promote abundance of *Akkermansia muciniphila*, an emerging probiotics in the gut, evidence from dietary intervention studies. J Funct Foods. 2017;33:194–201. [PubMed: 30416539]

45. Engevik MA, Ruan W, Esparza M, Fultz R, Shi Z, Engevik KA, et al. Immunomodulation of dendritic cells by Lactobacillus reuteri surface components and metabolites. Physiol Rep. 2021;9:e14719. [PubMed: 33463911]

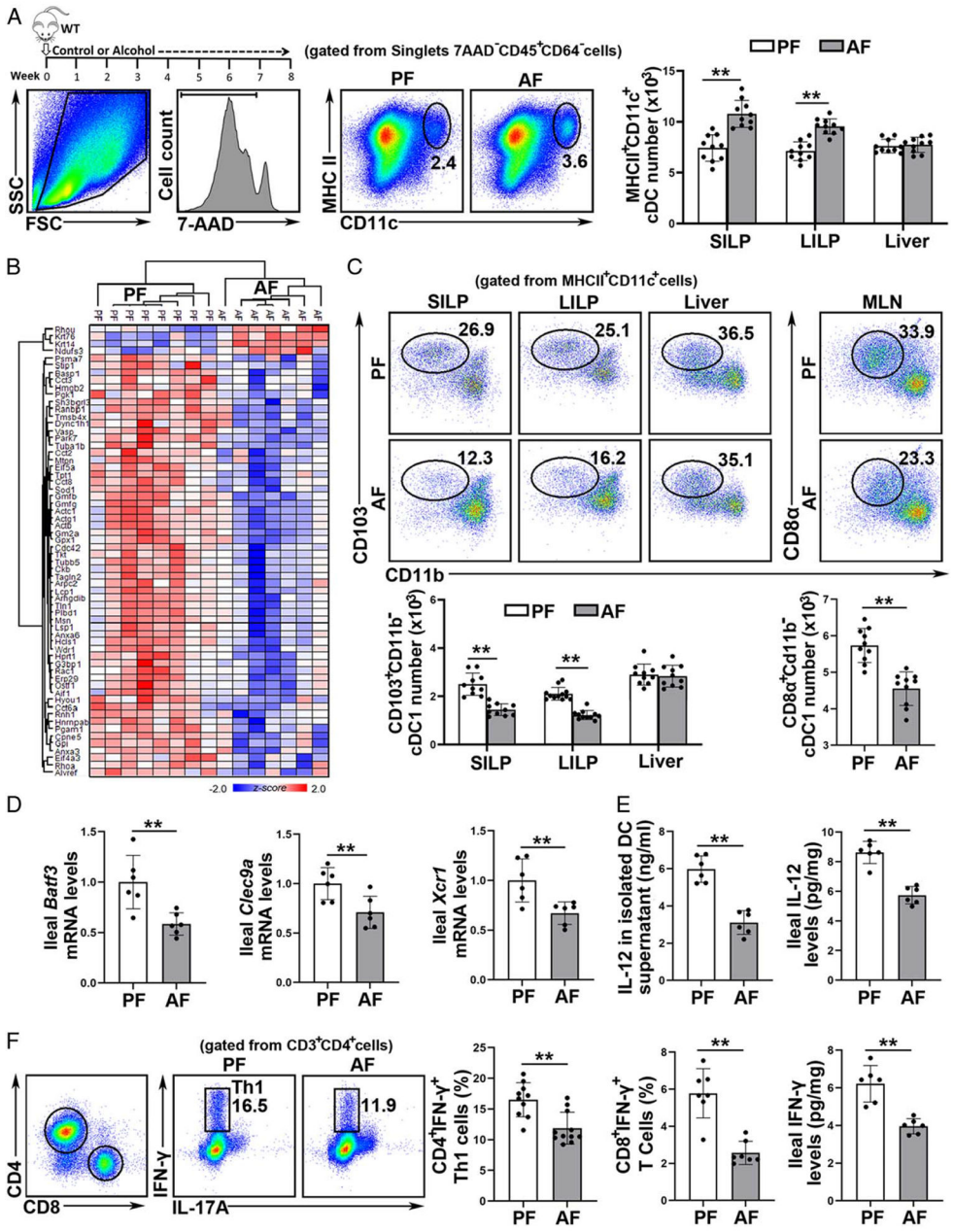

FIGURE 1.

Chronic alcohol consumption leads to a reduction of intestinal basic leucine zipper transcription factor ATF-like 3 (*Batf3*)-dependent conventional type 1 dendritic cells (cDC1s) in mice. C57BL/6J wild-type (WT) mice were fed Lieber-DeCarli liquid diets containing alcohol (alcohol-fed, AF) or isocaloric dextran (pair-fed, PF) for 8 weeks plus a single binge (4 g/kg). (A) Gating strategy and representative dot plot of singlet 7-AAD^{-}CD45^{+}CD64^{-}CD11c^{+}MHCII^{+} total cDCs (n = 10). (B) Heatmap plot of the proteomic changes of the purified ileal cDCs (n = 7–8). (C) Dot plot of intestinal cDC1s (n = 10). (D) Analysis of mRNA levels of ileal *Batf3*, *Clec9a*, and *Xcr1* (n = 6). (E) IL-12 levels quantified by ELISA (n = 6). (F) Th1 (CD3^{+}CD4^{+}IFN-γ^{+}) cells (n = 10),

$CD3^+CD8^+IFN\text{-}\gamma^+$ cells (n = 7), and protein interferon gamma (IFN-γ) levels (n = 6) in mouse ileum. Data are presented as mean ± SD. Statistical comparisons were made using Student *t* test; $^{**}P < 0.01$ versus PF mice.

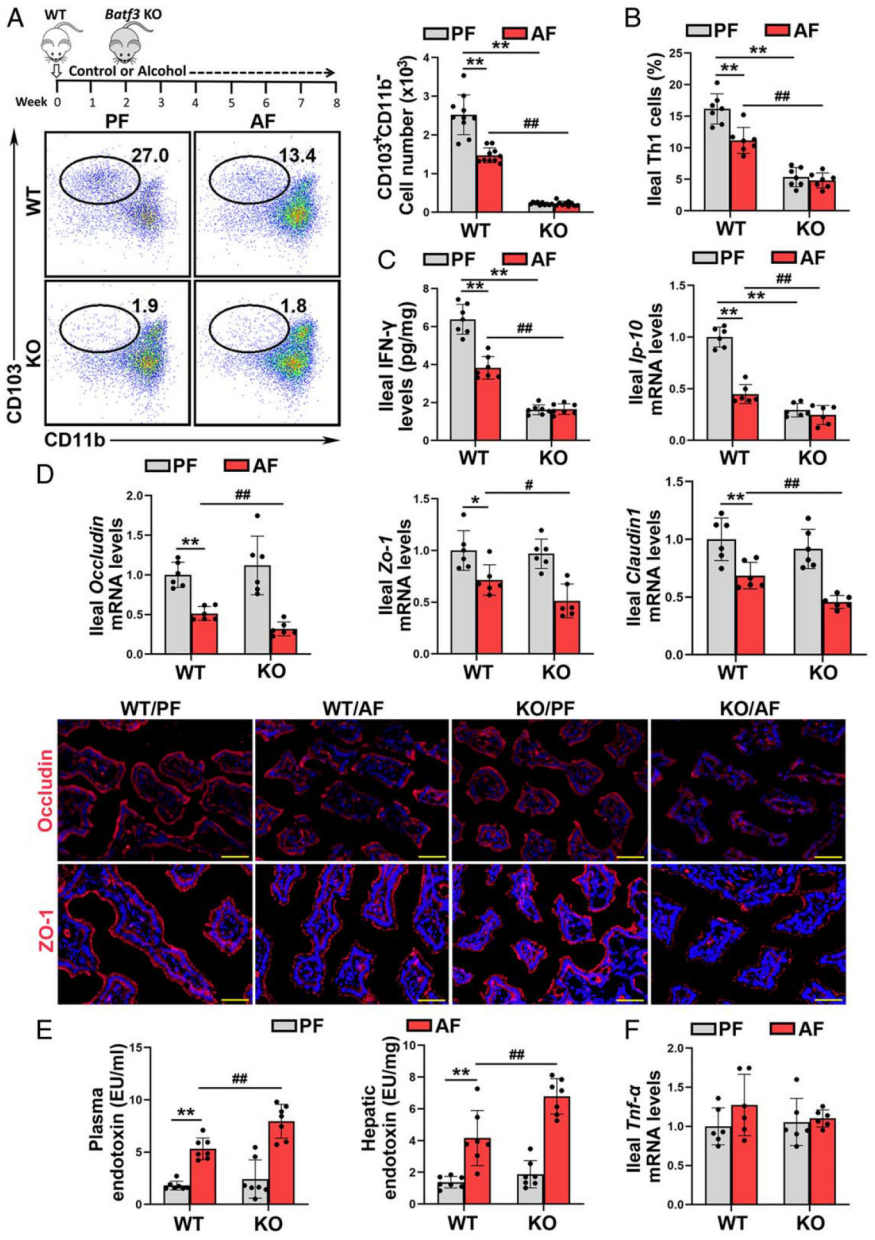

FIGURE 2.

Lack of basic leucine zipper transcription factor ATF-like 3 (*Batf3*)-dependent conventional type 1 dendritic cells (cDC1s) exacerbates alcohol-induced gut barrier disruption and pathogen-associated molecular patterns translocation into the liver. C57BL/6J wild-type (WT) mice and *Batf3*$^{-/-}$ mice were fed Lieber-DeCarli liquid diets containing alcohol or isocaloric dextran for 8 weeks plus a single binge (4 g/kg). (A) Dot plot of ileal cDC1s (n = 10). (B) Ileal Th1 cells proportion (n = 7). (C) Ileal interferon gamma (IFN-γ) protein levels (n = 7) and the mRNA levels of ileal *Ip-10* (n = 6). (D) The mRNA levels of ileal tight junctions (n = 6) and IF staining of ileal ZO-1 and OCCLUDIN (n = 6). (E) Plasma and hepatic LPS levels (n = 7). (F) Ileal *Tnf-α* mRNA levels (n = 6). Data are presented as mean

± SD. *$P < 0.05$, **$P < 0.01$ versus WT/PF mice; $^{\#}P < 0.05$, $^{\#\#}P < 0.01$ versus WT/AF mice. AF, alcohol-fed; PF, pair-fed; LPS, lipopolysaccharide.

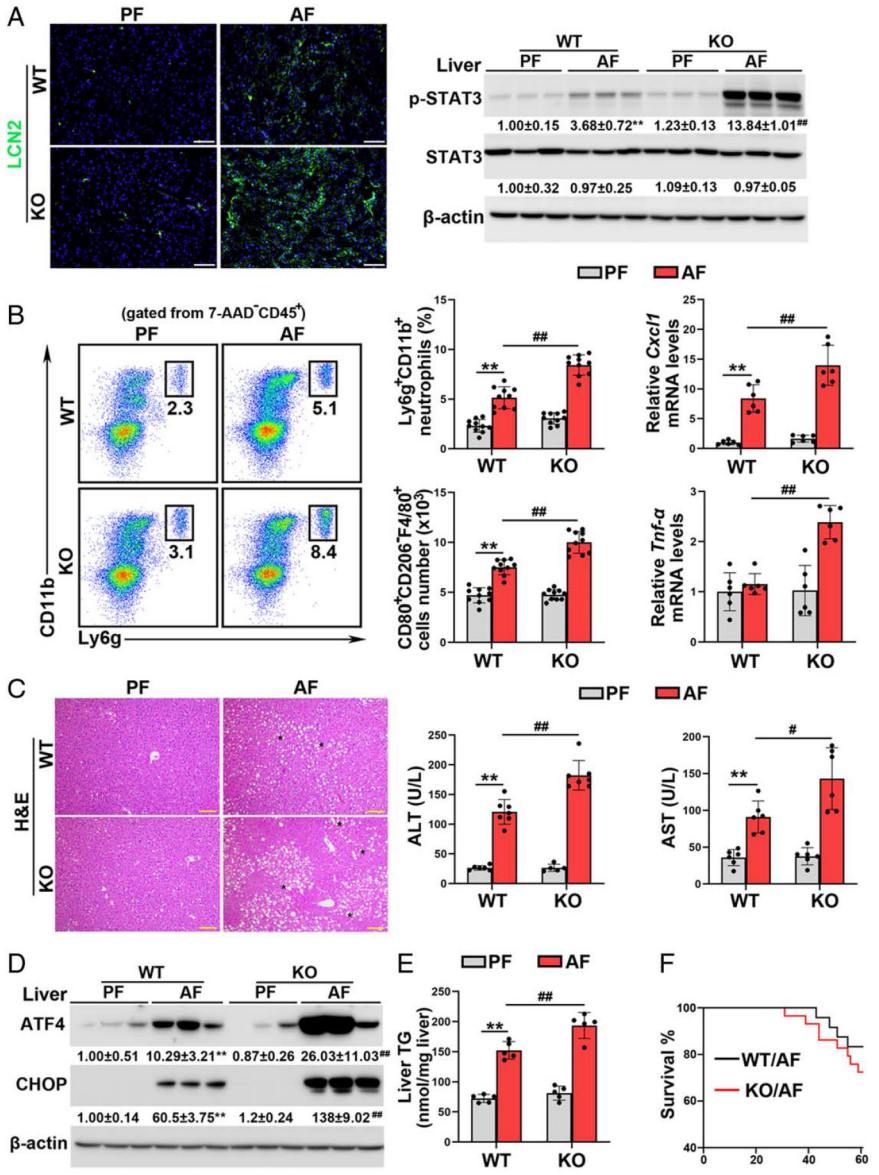

FIGURE 3.

The alcohol-induced hepatic inflammatory, steatosis, and ER stress were exacerbated in basic leucine zipper transcription factor ATF-like 3 (*Batf3*$^{-/-}$) mice. (A) IF staining of lipocalin-2 (LCN2) (n = 7) and western blot analysis of p-signal transducer and activator of transcription 3 (STAT3) and STAT3 (n = 3) in the liver. (B) Hepatic neutrophils (n = 10), M1 macrophages (n = 10), and the mRNA levels of hepatic C-X-C Motif Chemokine Ligand 9 (*Cxcl1*) and *Tnf-α* (n = 6). (C) Liver hematoxylin and eosin (H&E) staining and plasma alanine aminotransferase (ALT) and aspartate aminotransferase (AST) activities (n = 5–7). Scale bars: 50 μm. Asterisks: lipid droplets. (D) Western blot analysis of hepatic activating transcription factor 4 (ATF4) and C/EBP homologous protein (CHOP) (n = 3). (E) Hepatic TG contents (n = 5). (F) Mouse survival rate. Data are presented as mean ± SD. $^{**}P < 0.01$ versus wild-type (WT)/pair-fed (PF) mice; $^{\#}P < 0.05$, $^{\#\#}P < 0.01$ versus WT/alcohol-fed (AF) mice. ER indicates endoplasmic reticulum; IF, immunofluorescence; TG, triglyceride.

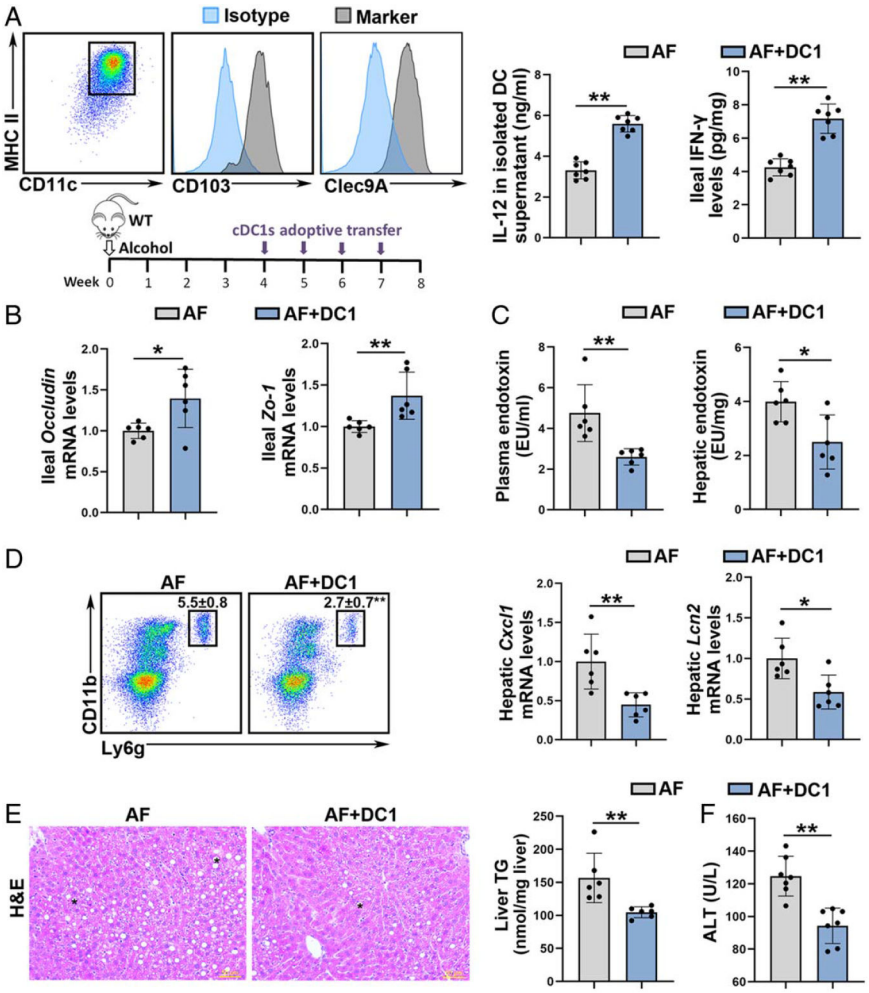

FIGURE 4.

Adoptive transfer of conventional type 1 DCs (cDC1s) recovered alcohol-induced *Akkermansia muciniphila* abundance reduction and liver injury in mice. Alcohol-fed C57BL/6J wild-type (WT) mice were administrated with or without cDC1s adoptive transfer. (A) cDC1 were specific and efficiently generated. IL-12 protein levels in isolated DCs and ileal interferon gamma (IFN-γ) protein levels (n = 7). (B) The mRNA levels of ileal *Occludin* and *Zo-1* (n = 6). (C) Plasma and hepatic LPS levels (n = 6). (D) Representative dot plot and frequency of neutrophils in the liver (n = 6). The mRNA levels of hepatic *Cxcl1* and *Lcn2* (n = 6). (E) Liver hematoxylin and eosin (H&E) staining and hepatic TG contents (n = 6). Scale bars: 50 μm. Asterisks: lipid droplets. (F) Plasma alanine aminotransferase (ALT) levels (n = 7). Data are presented as mean ± SD. Statistical comparisons were made using Student *t* test. **P* < 0.05, ***P* < 0.01 versus alcohol-fed (AF) mice. LPS indicates lipopolysaccharide; TG, triglyceride.

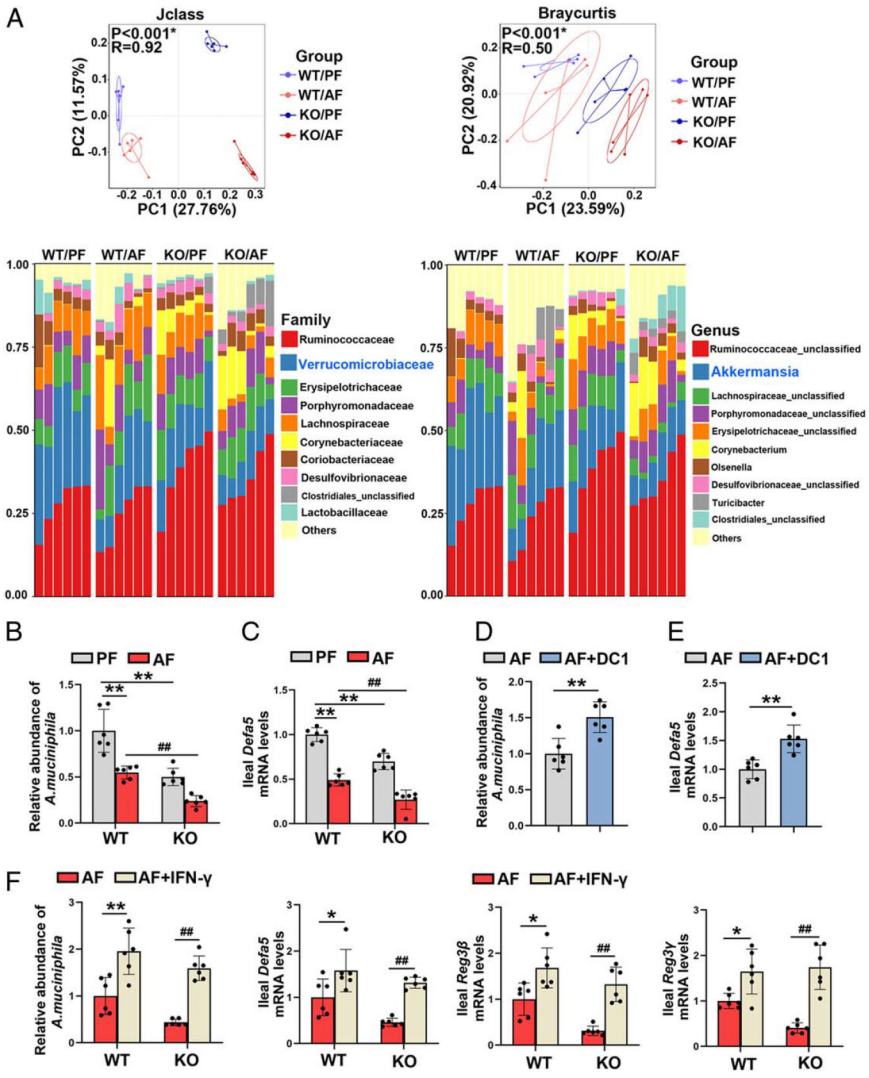

FIGURE 5.

Lack of conventional type 1 DCs (cDC1) in gut exacerbated alcohol-reduced *Akkermansia muciniphila* abundance. (A–C) C57BL/6J wild-type (WT) mice and *Batf3*$^{-/-}$ mice were fed Lieber-DeCarli liquid diets containing alcohol or isocaloric dextran for 8 weeks plus a single binge (4 g/kg). (A) PCoA plot showing dissimilarity in bacterial community structures based on J-class and Bray-Curtis distances, respectively (n = 6). Barplot showing the cecal bacterial compositions at the family level (left) and genus (right) level, respectively (n = 6). (B) Relative ileal *A. muciniphila* abundance (n = 6). (C) The mRNA levels of ileal Defa5 (n = 6). (D–E) Alcohol-fed C57BL/6J WT mice were administrated with or without cDC1s adoptive transfer. (D) Relative ileal *A. muciniphila* abundance (n = 6). (E) The mRNA levels of ileal Defa5 (n = 6). (F) Alcohol-fed C57BL/6J WT mice and *Batf3*$^{-/-}$ mice were administrated with or without interferon gamma (IFN-γ), respectively. (F) Relative *A. muciniphila* abundance and the mRNA levels of ileal antimicrobial peptides (AMPs) (n = 6). In panels A–C, data are presented as mean ± SD. $^{**}P < 0.01$ versus WT/pair-fed (PF) mice; $^{\#}P < 0.05$, $^{\#\#}P < 0.01$ versus WT/AF mice. In panels D and E, data are presented as mean

± SD. $^{**}P < 0.01$ versus alcohol-fed (AF) mice. In panel F, data are presented as mean ± SD. $^{*}P < 0.05$, $^{**}P < 0.01$ versus WT/AF mice; $^{\#\#}P < 0.01$ versus knockout (KO)/AF mice. PCoA, principal coordinates analysis.

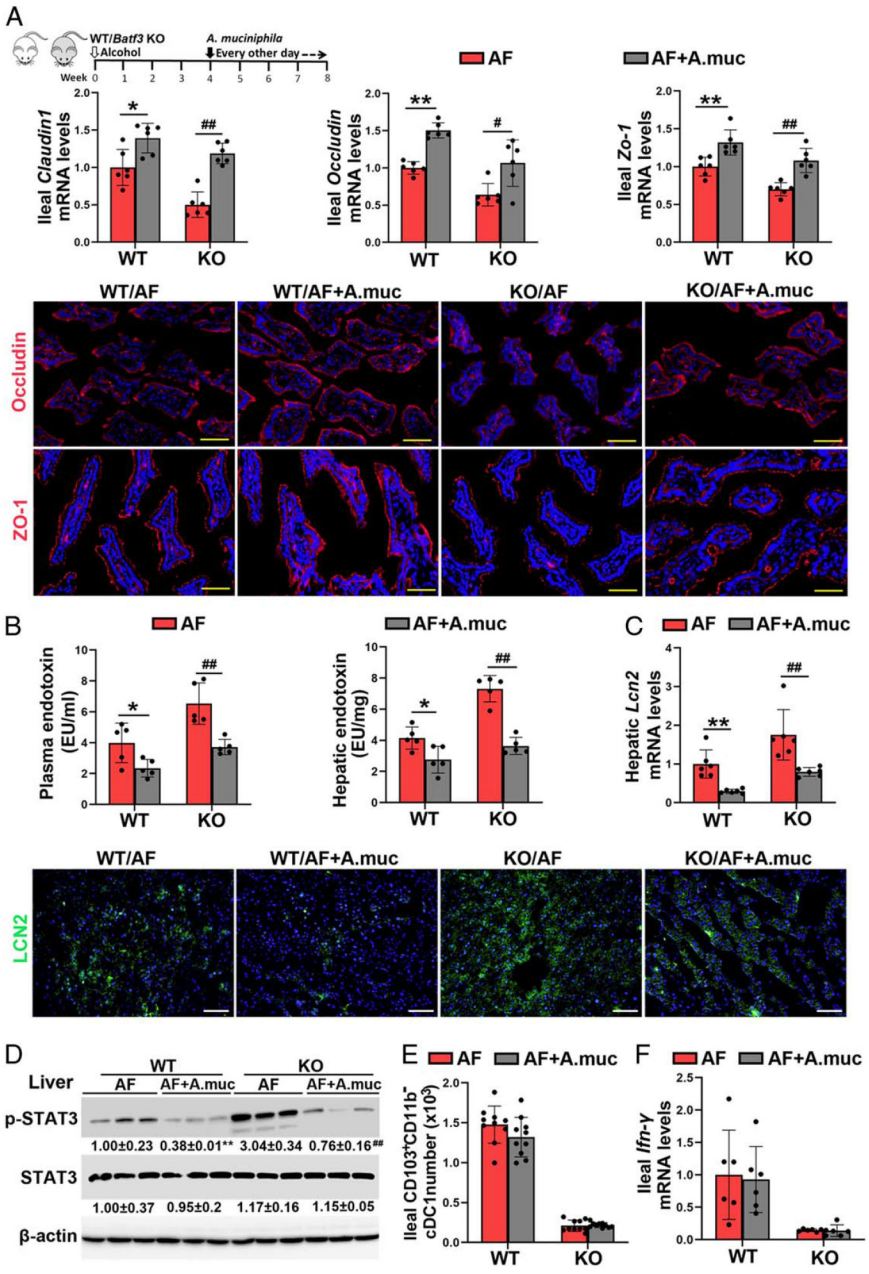

FIGURE 6.

Akkermansia muciniphila supplementation ameliorated alcohol-induced tight junction disruption and pathogen-associated molecular patterns (PAMPs) translocation in both wild-type (WT) mice and *Batf3*$^{-/-}$ mice. Alcohol-fed C57BL/6J WT mice and *Batf3*$^{-/-}$ mice were administrated with or without *A. muciniphila*, respectively. (A) The mRNA levels of ileal *Zo-1*, *Occludin*, and *Claudin1* (n = 6) and the IF staining of ileal ZO-1 and OCCLUDIN. Positive signals of ZO-1 and OCCLUDIN were stained in red, respectively, while nuclei were stained by DAPI in blue. Scale bar, 50 μm. (B) Plasma and hepatic LPS levels (n = 5). (C) The mRNA levels and protein levels of hepatic lipocalin-2 (LCN2) (n = 6). Positive signals of LCN2 were stained in green, while nuclei were stained by DAPI

in blue. Scale bar, 50 μm. (D) Hepatic protein levels of p-signal transducer and activator of transcription 3 (STAT3) and STAT3 (n = 3). (E) The numbers of ileal $CD103^{+}CD11b^{-}$ cDC1s (n = 10). (F) Relative ileal *Ifn-γ* mRNA levels (n = 6). Data are presented as mean ± SD. $^{*}P < 0.05$, $^{**}P < 0.01$ versus WT/alcohol-fed (AF) mice; $^{\#}P < 0.05$, $^{\#\#}P < 0.01$ versus knockout (KO)/AF. DAPI, 4′,6-diamidino-2-phenylindole IF, immunofluorescence; LPS, lipopolysaccharide.

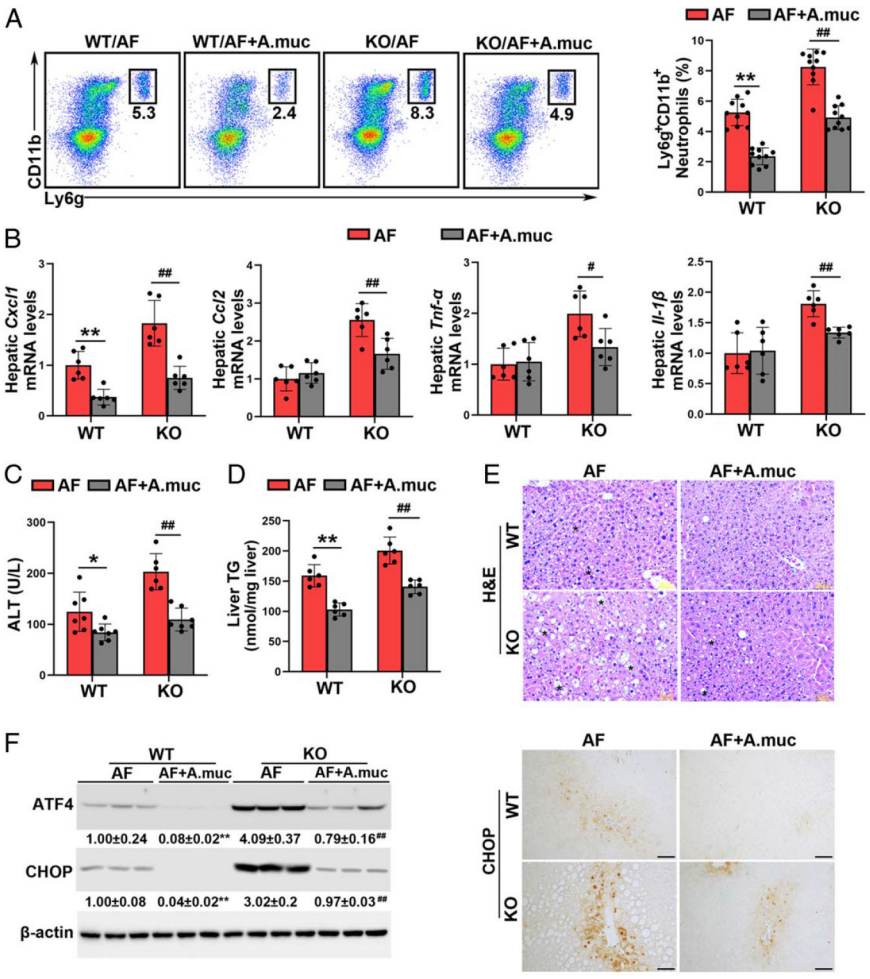

FIGURE 7.

Akkermansia muciniphila administration protects against alcohol-induced liver injury in both wild-type (WT) mice and *Batf3*$^{-/-}$ mice. Alcohol-fed C57BL/6J WT mice and *Batf3*$^{-/-}$ mice were administrated with or without *A. muciniphila*, respectively. (A) Representative dot plot and frequency of neutrophils in the liver (n = 10). (B) The mRNA levels of hepatic *Cxcl1*, *Ccl2*, *Tnf-α*, and *Il-1β* (n = 6). (C) Plasma alanine aminotransferase (ALT) levels (n = 6–7). (D) Hepatic TG contents (n = 6). (E) Liver histopathological changes are shown by hematoxylin and eosin (H&E) staining. Scale bars: 50 μm. Asterisks: lipid droplets. (F) Hepatic ATF4 and CHOP protein levels (n = 3) and IHC staining of hepatic CHOP. Scale bars: 50 μm. Data are presented as mean ± SD. *$P < 0.05$, **$P < 0.01$ versus WT/alcohol-fed (AF) mice; $^{\#}P < 0.05$, $^{\#\#}P < 0.01$ versus knockout (KO)/AF. IHC, immunohistochemistry; TG triglyceride.

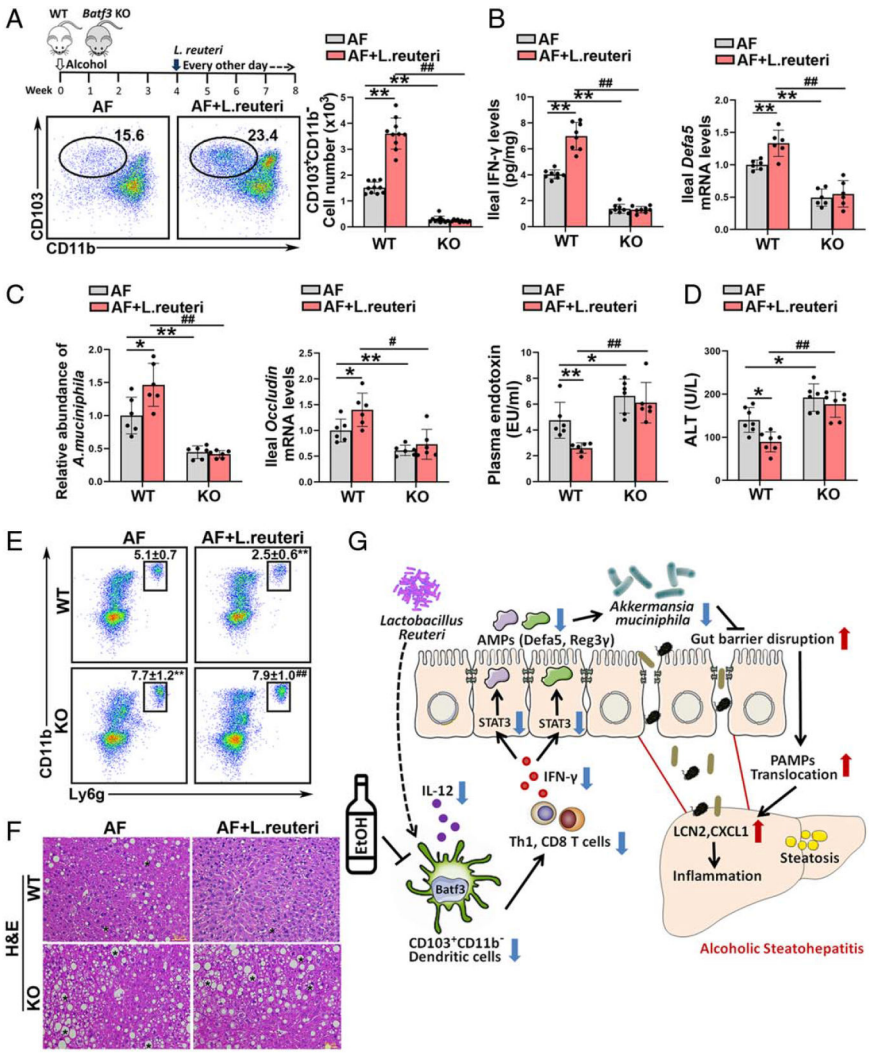

FIGURE 8.

Intestinal conventional type 1 DCs (cDC1s) are required for the protective role of *Lactobacillus reuteri* in alcohol-induced steatohepatitis. Alcohol-fed C57BL/6J wild-type (WT) mice and *Batf3*$^{-/-}$ mice were administrated with or without *L. reuteri*, respectively. (A) The dot plot and relative frequency of ileal CD103^{+}CD11b^{-} cDC1s (n = 10). (B) Ileal interferon gamma (IFN-γ) protein levels (n = 8) and the ileal mRNA levels of *Defa5* (n = 6). (C) Relative *A. muciniphila* abundance (n = 6), mRNA levels of ileal *Occludin* (n = 6), and plasma LPS levels (n = 6). (D) Serum alanine aminotransferase (ALT) levels (n = 7). (E) Representative dot plot and frequency of neutrophils in the liver (n = 10). (F) Liver histopathological changes shown by hematoxylin and eosin (H&E) staining. Scale bars: 50 μm. Asterisks: lipid droplets. (G) Summarized figure of this study. Data are presented as mean ± SD. *$P < 0.05$, **$P < 0.01$ versus WT/alcohol-fed (AF) mice; $^{\#}P < 0.05$, $^{\#\#}P < 0.01$ versus WT/AF+*L. reuteri*. LPS, lipopolysaccharide.